

THE VOYAGER MISSION PHOTOPOLARIMETER EXPERIMENT

CHARLES F. LILLIE and CHARLES W. HORD

*Laboratory for Atmospheric and Space Physics and Department of Astro-Geophysics,
University of Colorado at Boulder, Boulder, Colo. 80309, U.S.A.*

KEVIN PANG

Planetary Science Institute, Pasadena, Calif. 91101, U.S.A.

and

DAVID L. COFFEEN and JAMES E. HANSEN

Goddard Institute for Space Studies, New York, N.Y. 10025, U.S.A.

(Received 24 May, 1977)

Abstract. The Voyager Photopolarimeter Experiment is designed to determine the physical properties of particulate matter in the atmospheres of Jupiter, Saturn, and the Rings of Saturn by measuring the intensity and linear polarization of scattered sunlight at eight wavelengths in the 2350–7500 Å region of the spectrum. The experiment will also provide information on the texture and probable composition of the surfaces of the satellites of Jupiter and Saturn and the properties of the sodium cloud around Io. During the planetary encounters a search for optical evidence of electrical discharges (lightning) and auroral activity will also be conducted.

1. Introduction

The primary scientific objectives of the photopolarimeter experiment on the Voyager mission may be divided into two categories: (1) the study of the atmospheric properties of Jupiter, Saturn, Titan, and other satellites that may have thin atmospheres; and (2) the study of the surface properties of the satellites of Jupiter and Saturn which have little or no atmosphere. Saturn's Rings may be expected to involve aspects of both categories in that the Rings may contain small amounts of fine particulate matter, as do the atmospheres of the planets, as well as being an ensemble of small satellites whose surface properties are to be studied. Investigation of the sodium emission associated with Io has implications about both the surface and atmospheric (ionospheric) properties of Io, as well as the magnetic field and charged particle environment of the Jovian system. The search for auroral emissions on the dark sides of Jupiter and Saturn provides both magnetic field and charged particle information, as well as atmospheric data.

Specific scientific objectives associated with the atmospheres of Jupiter, Saturn, and Titan are:

(1) to determine the vertical distribution of cloud particles (atmospheric aerosols) down to an optical depth of unity, using intensity and polarization measurements as a function of viewing angle and wavelength (i.e., to define the macrostructure of the clouds).

(2) to use measurements of the scattering and polarizing efficiency of the effective cloud particle as a function of phase angle and wavelength to obtain information on the particle size, shape, and probable composition. (These measurements define the microstructure of the clouds.)

(3) to achieve the first two objectives, determination of cloud micro- and macro-structures, for the major features of the planets such as the Red Spot of Jupiter and the zones, belts, and polar regions on Jupiter and Saturn.

(4) to use polarization measurements at large phase angles to confirm or reject the presence of regular crystalline particles of the particle shape/refractive index combinations predicted as possible cloud compositions. In cases where polarization measurements indicate the presence of spherical particles, refractive index may be determined as well as size distribution so that probable particle composition may be determined.

(5) to use the results of the above studies to provide correct inputs for the effects of particulate scattering and absorption on thermal balance and model calculations for these atmospheres.

Specific scientific objectives associated with the satellites are:

- (6) to measure or set upper limits on the density of their atmospheres.
- (7) to determine the texture and probable composition of their surfaces.
- (8) to determine the bond albedo of each satellite.
- (9) to map the distribution of sodium vapor in the vicinity of Io and in the Jovian magnetosphere.

Specific scientific objectives for the study of Saturn's Rings are –:

(10) to use measurements of the intensity and polarization of light scattered by Saturn's Rings as a function of wavelength and viewing angle to provide information on the size, shape, and probable composition of the ring particles, as well as their density and radial distribution.

(11) to use observations of the extinction and scattering of starlight to give additional information on particle size and ring optical depth.

(12) to use the results of the above studies to provide information on the ring particle dynamics: alignment forces, particle lifetimes, and the gravitational field of Saturn.

2. Instrumentation

HARDWARE

The Voyager Photopolarimeter Experiment (PPS) utilizes a general purpose filter photometer/polarimeter which has been optimized for the encounter phase of the mission. The instrument (Figure 1) consists of a 6-inch, $f/1.4$, Dahl-Kirkham-type, Cassegrain telescope; a four-position aperture wheel that provides 1/16, 1/4, 1, and 3.5 degree diameter circular fields-of-view (FOV); an eight-position analyzer wheel

with open, dark, and calibration source positions, plus five polacoat analyzers with their transmitting axes located at 0, 60, 120, 45, and 135 degrees rotation; an eight-position filter wheel with thin film interference filters; and an EMR 510-E-06 photomultiplier tube (PMT) with a tri-alkali (S-20) photocathode. The effective wavelength of each filter, its nominal band width, typical instrumental sensitivities, and the particular atomic and molecular species to which it is sensitive are listed in Table I. Individual photon events in the PMT are detected with pulse-counting electronics.

The wide dynamic range required by the Voyager mission (4 to $6 \times 10''$ photon $\text{cm}^{-2} \text{sec}^{-1} \text{\AA}^{-1} \text{ster}^{-1}$) can be accommodated by FOV changes and an electronic gain change in the PMT which reduces the instrumental sensitivity by a factor of approximately 50.

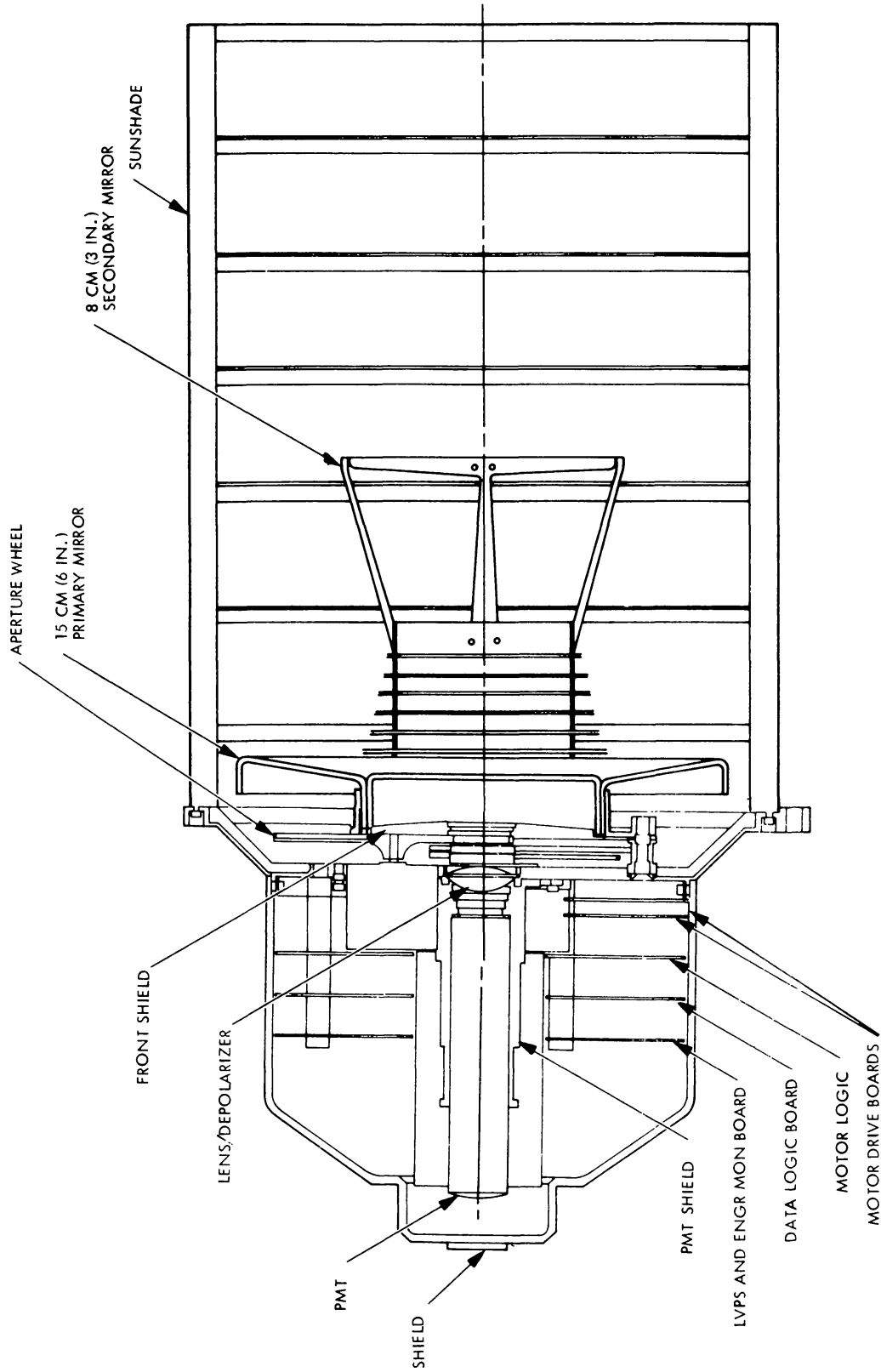
The basic instrument weighs 2.55 kg, including 0.78 kg of tungsten and aluminum shielding to protect critical components from trapped radiation in the Jovian magnetosphere where the flux may exceed 10^8 3 MeV equivalent electrons $\text{cm}^{-2} \text{s}^{-1}$. A shadow caster (not shown) prevents direct sunlight from entering the aperture of the instrument for phase angles $< 160^\circ$. A solar sensor has been provided to turn the high voltage off if the PPS is pointed within 20 degrees of the Sun.

In-flight calibration of the experiment will be accomplished by observing a set of standard stars of known brightness and polarization; the sunlight scattered by an on-board calibration target (unpolarized light); and the light from stars and the planets reflected into the PPS from a mirror tilted to the Brewster angle (100% polarized light). An internal, Cl_{36} , Cerenkov, radiation source mounted on the analyzer wheel provides a short-term measure of the instrument's stability.

The instrument is capable of measuring the polarization of the planets and their satellites with a precision of $\pm 0.5\%$ and their relative brightness with an accuracy of ± 0.5 to 1.0% . Its absolute calibration should be known to ± 2 or 3% in the visible and infrared and $\pm 10\%$ in the ultraviolet. For measurements of low surface brightnesses the instrument's sensitivity ranges from ~ 140 counts/Rayleigh in the visible and UV to ~ 20 counts/Rayleigh in the infrared.

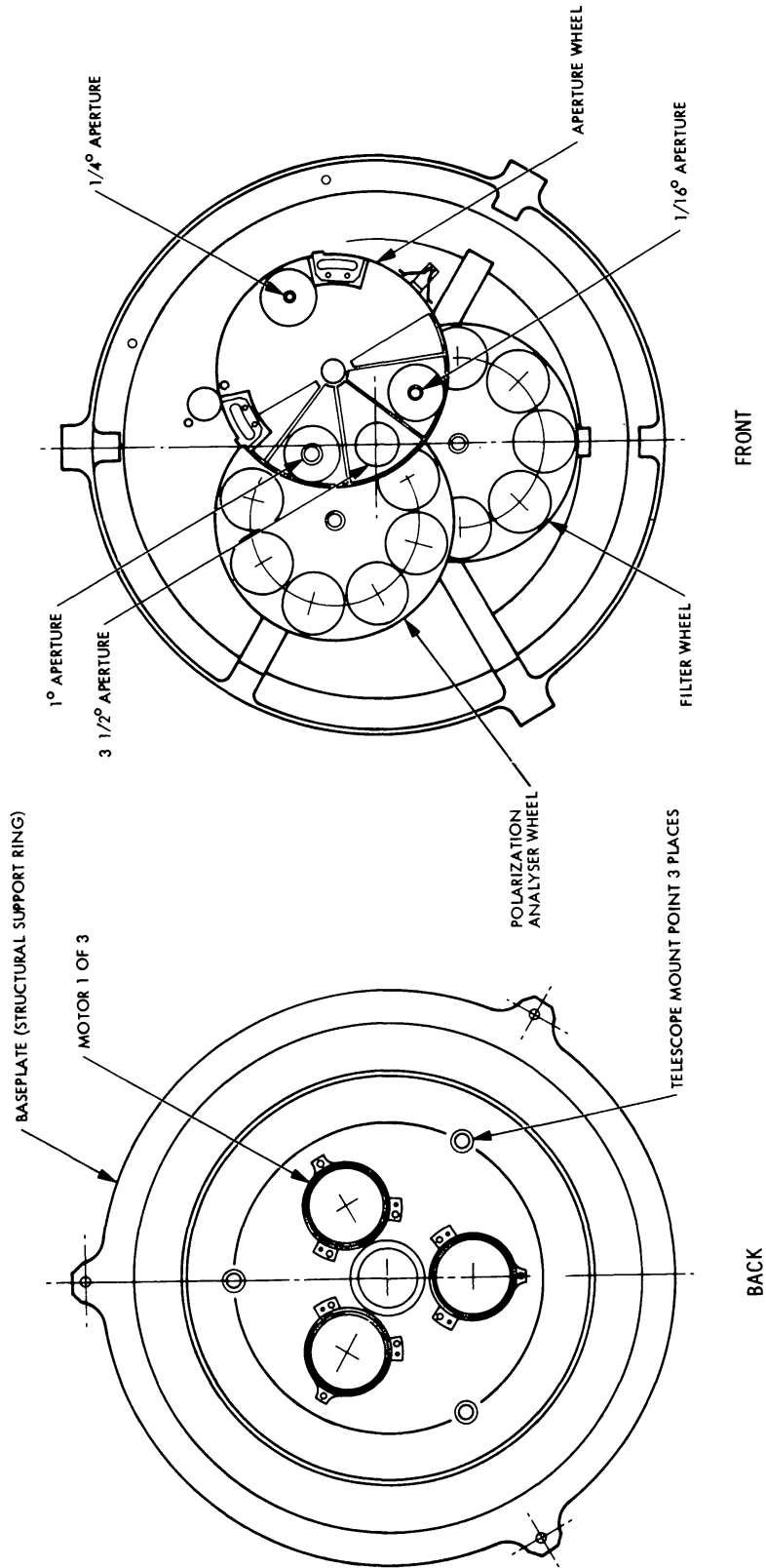
The normal operational (encounter) mode of the PPS is to step through a programmed sequence of 40 filter/analyzer wheel combinations once every 24 sec. Each measurement consists of a 400 millisecond (ms) integration period followed by a 200 ms period during which the next filter or analyzer is stepped into place. A measurement set consists of readings in the open, 0° , 60° , 120° , and dark positions of the analyzer wheel for each of the eight filters. From these data the I , Q , and U Stokes parameters can be derived. No attempt is made to measure the V vector which is of order 10^{-3} to 10^{-4} in most cases.

For stellar occultation and satellite eclipse measurements, the experiment may be operated with the filters and analyzers fixed in position and a 10 ms integration period. This 'occultation' mode provides rapid measurements in order to resolve spikes in the light curves due to turbulence in the occulting planet's atmosphere, as seen in Earth-based observations. The measurement sequence can be modified



Photopolarimeter Configuration

Fig. 1a. A cross-sectional view of the Photopolarimeter Experiment.



Photopolarimeter Configuration (Electronics and Mirrors Removed)

Fig. 1b. Front and back views of the PPS base plate showing the motor placement and filter, analyzer, and aperture wheel arrangement.

TABLE I

Position number	Filter characteristics			Spectral features
	Effective wavelength (Å)	Half-power bandwidth (Å)	Nominal sensitivity ^a	
1	5900	100	30	Sodium D
2	4900	100	50	Hydrogen H _β
3	3900	100	45	Helium I, Ca II
4	3100	300	40	OH Emission
5	2630	300	25	Ozone, Chromophore, Mg II
6	2350	300	20	Rayleigh Scattering, Si I
7	7500	300	8	Aerosol Scattering, K I
8	7270	100	4	CH ₄ Absorption Band

^a For a point source in counts accumulated during an 0.4 sec integration per incident photon $\text{cm}^{-2} \text{sec}^{-1} \text{Å}^{-1}$.

during flight by changing the PPS look-up-table in the spacecraft's Flight Data System (FDS). During interplanetary cruise the 400 ms integration time will be increased to as much as 36 sec due to the low data rates which are available with the S-Band transmitter when the spacecraft is beyond the orbit of Saturn.

The PPS data readout consists of a 30-bit digital word, of which 20 bits provide the data count accumulated during the integration period, and 10 bits indicate instrument status. In order to reduce the telemetry rate the PPS data count bits are log compressed to 14 bits (10 bit mantissa and 4 bit exponent). The nominal data rate of the PPS experiment is, thus, 40 bps, with a maximum of $1023\frac{1}{2}$ bps and a minimum of 0.6 bps.

POLARIZATION DETERMINATION

Four Stokes' parameters, I , Q , U , and V , completely specify the state of polarization of a quasi-monochromatic wave. The advantages of measuring and using Stokes' parameters are: (1) they all have the same dimension of intensity; (2) they are additive and, therefore, most conveniently suited for analytical treatment; and (3) from the Stokes' parameters we can generate the degree and plane of polarization and ellipticity.

Wolstencroft and Rose (1967) observed that the degree of ellipticity, $e = V/I$, of the zodiacal light is on the order of 1%. Swedlund *et al.* (1972) found that the circular polarization of Jupiter and Saturn is very small ($e \approx 10^{-4}$). Since the measurement of V requires a much more complex instrument and is not necessary to meet the objectives of this experiment, only I , Q , and U will be determined.

The plane of polarization of light, specified by the angle $\zeta = \frac{1}{2} \arctan(U/Q)$, singly scattered from Rayleigh particles is perpendicular to the scattering plane. Multiple scattering, scattering from aerosol particles (especially those of irregular shape), and reflection from surfaces can create odd orientations of the plane of polarization.

Therefore, measurements of U can give additional information on aerosol and surface properties and the importance of multiple scattering.

We can measure the total intensity, I , either with no polarizer in the optical train, or by summing three intensities measured through polarizers with their transmission axes at 0° , 60° , and 120° :

$$I = 2[I(0^\circ) + I(60^\circ) + I(120^\circ)]/3.$$

The Stokes' parameter Q is given by

$$Q = 2[2I(0^\circ) - I(60^\circ) - I(120^\circ)]/3.$$

Similarly, U can be determined from:

$$U = 2[I(60^\circ) - I(120^\circ)]/\sqrt{3}.$$

Thus, with three intensity measurements we can determine all three Stokes' parameters. The degree of polarization is calculated as follows:

$$P = \frac{[Q^2 + U^2]^{1/2}}{I}.$$

In this manner we will be able to measure the degree of polarization at eight wavelengths with a precision of better than 0.5%. With the phase angle coverage that can be obtained from the Voyager spacecraft, we expect to observe polarizations in the 10's of percent (0 to 72% for Jupiter from Pioneer observations) for atmospheres and up to 60% for satellite surfaces. These data will be sufficient for the derivation of both gross cloud structure and the microstructure of cloud particles and visible planetary surfaces. Higher accuracy would require unacceptable penalties in weight and cost.

3. Observations

The observations necessary to achieve the scientific objectives fall into two general classes, depending upon whether the observed body underfills or overfills the instrument's field of view. In the case where the field of view is underfilled, as will be true for most satellite observations, intensity and polarization for each wavelength interval are measured as a function of a single variable, phase angle.

In cases where the body being observed has an atmosphere, phase angle observations at intervals of 5° or less will be made in order to determine atmospheric particle properties. The phase measurement for regular particles, spherical or crystalline, provide the opportunity for unique identification. When the field of view is underfilled, these atmospheric observations are similar to those made of Venus from Earth.

When the planet or satellite overfills the instrument field of view, reference must be made to a coordinate system as shown in Figure 2. The geometry for photopolarimeter observations is specified by the angles of incident and scattered

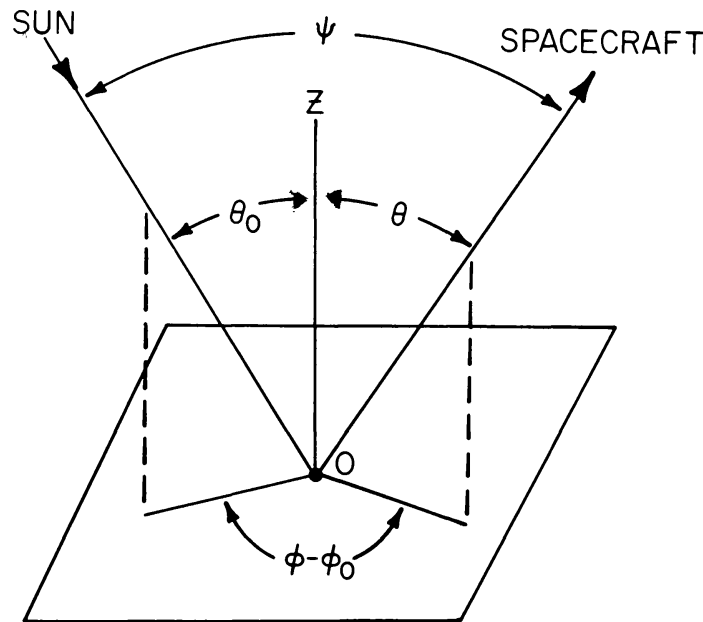


Fig. 2. The geometry for PPS observations. Z is the normal to the surface, while θ_0 and θ are the angles of incidence and reflectance, ψ is the phase angle, and $\psi - \psi_0$ is the azimuthal angle.

radiation $\mu_0 \equiv \cos \theta_0$, $\mu \equiv \cos \theta$, and either the azimuthal angle $\phi - \phi_0$ or the phase angle ψ . In cases of oblique viewing or oblique solar illumination, i.e., when μ or μ_0 is sufficiently small, atmospheric curvature effects become important and different variables are necessary. Observations near the terminator or bright limb as well as stellar occultation measurements are examples of curvature geometries. The origin of this coordinate system on the measured body is defined by latitude, longitude, and time in the case of planets and satellites. For Saturn's Rings, radial distance from Saturn's center, azimuthal angle, and time specify the measurement location. In case of extreme curvature geometries for bodies with atmospheres, it is also necessary to specify the altitude of observation.

Measurements of scattered intensity and polarization as a function of phase angle, necessary to determine individual cloud particle properties or microstructure, are time-critical in nature. This is true since a given object can be viewed at a specific phase angle only at specific times during the mission. For example, the phase angle variation for Jupiter, during the course of a typical planned trajectory, is shown in Figure 3. During close encounter the determination of the scattered intensity and polarization as a function of observer zenith angle, which is necessary to find the vertical distribution of cloud particles or macrostructure, is accomplished by moving the photopolarimeter field of view in the ('pitchfork') pattern illustrated in Figure 4. This observational pattern provides the required zenith angle coverage, a survey of all latitudes, and coordination with prime observations of other scan platform instruments (particularly the infrared spectrometer measurements). Since many other scan platform observational activities will be carried on during the near encounter time period, this pattern can only be performed three times for each spacecraft during an encounter. In order to complete the phase angle observations

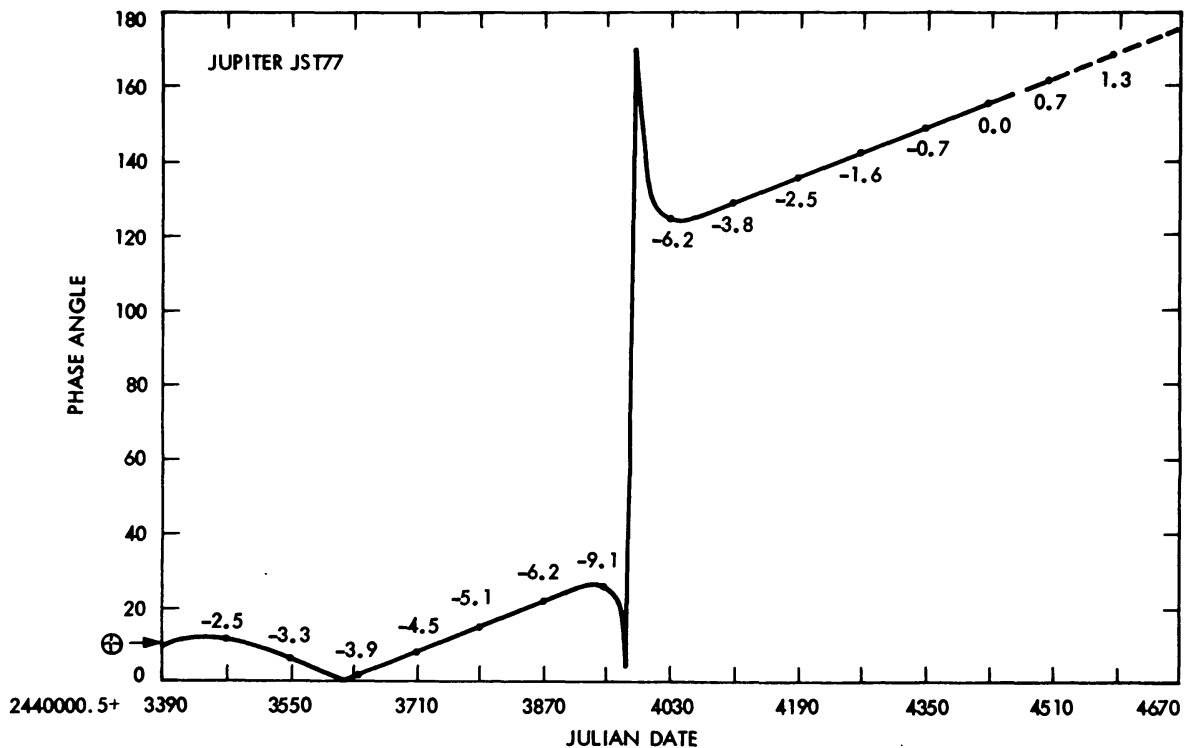


Fig. 3. Variation of phase angle versus time for viewing Jupiter from the Voyager spacecraft. The maximum phase angle observable from Earth is 12°. The curve is labelled with the visual brightness of the planetary disk in astronomical magnitudes. The shape of the phase angle curve is similar for prograde passage of Saturn and other bodies.

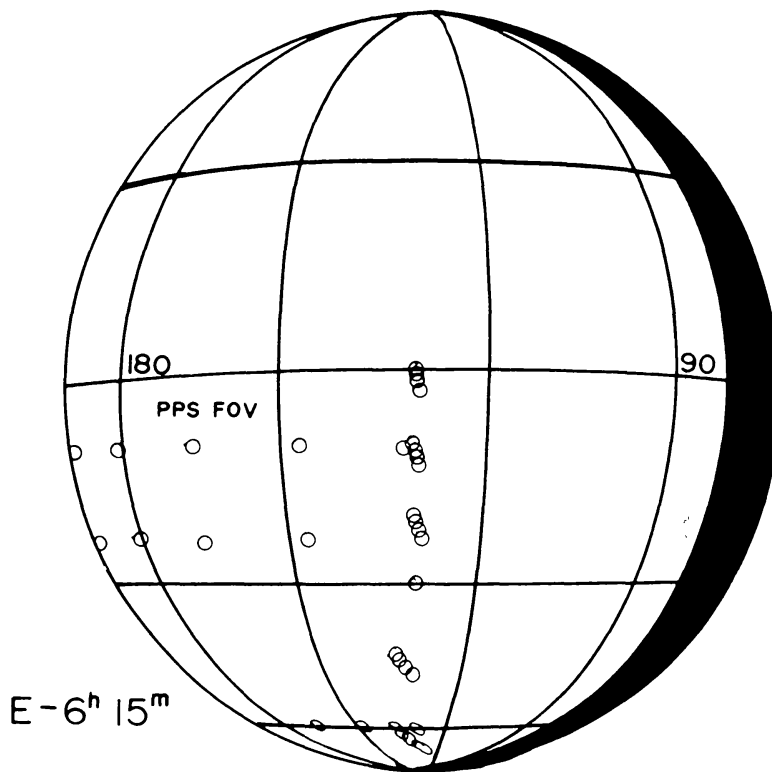


Fig. 4. Scan platform pattern required to incorporate PPS constant latitude scans along belts and zones, plus North-South scanning. Repetitive use of this pattern will provide the necessary zenith angle and phase angle coverage.

1977SRV...21...159L

for every 5° of change, coordinated observations will be performed with the imaging experiment in order to view the same types of features as in the 'pitchfork' pattern at missing phase angles. Coordinated 'feature following' measurements with the imaging experiment provide spacecraft zenith angle and illumination angle variation and will help in the solution for vertical cloud structure. In 'feature following' observations, phase angle and zenith angle variations are highly correlated, necessitating the use of the 'pitchfork' pattern to successfully separate cloud macrostructure and microstructure scattering effects.

For Jupiter, the constant-latitude scans in the 'pitchfork' pattern will be along the zone containing the Red Spot and along an equatorial belt. With this scheme very dense zenith angle and phase angle coverage will be obtained for the belt and zone, assuming horizontal homogeneity. Groundbased studies indicate the belt and zone features on Jupiter can break into smaller features, with loss of the identity of specific zones and belts. If this proves to be the case, polarization data will give average properties at these characteristic latitudes in the same way that average cloud particle properties are obtained for Venus when the full disk is observed. With detailed information obtained for the two observed latitudes, it will be possible to relate this information to other latitudes by means of North-South scans. Moreover, by proper timing of the observations, phase angle and zenith angle coverage will be included, in the course of this pattern, for a few specific local regions on the planet.

Use of bright limb (small μ) and terminator (small μ_0) geometries extends the level above which scattering and absorbing properties are measured high in the atmosphere. The significant variable is the airmass factor, $1/\mu + 1/\mu_0$. As the airmass increases, i.e., as μ and/or μ_0 decrease, the intensity and polarization measurements are characteristic of atmospheric particle properties higher in the atmosphere.

Stellar occultation measurements provide the light curve of a star or distant planet, e.g., Venus, as it sets or rises through the atmosphere of Jupiter, Saturn, or Saturn's Rings. These measurements provide a special geometry with large airmass and forward scattering, ($\psi \approx 180^\circ$). The stellar occultation technique will be used at Saturn and possibly at Jupiter, depending upon the extent of charged particle interference.

As applied to a planetary atmosphere, the slope of the occultation light curve at the occultation (half intensity) point, provides a measure of the temperature at the occultation point pressure level. Extinction or light defocusing effects of atmospheric particulate matter above the occultation pressure produce rapid fluctuations in the light curve, superimposed on the general decrease in light intensity. Use of a planet such as Venus as an occultation light source having an extent comparable to an atmospheric scale height will help separate out turbulence effects which have plagued the interpretation of this type of data. If the turbulence is not saturated, the use of stellar as well as extended planet light sources will provide the opportunity to measure the scale size of turbulent effects.

Stellar light sources will also be observed through Saturn's Rings. For these measurements the photopolarimeter will be pointed directly at a star and the light

curved will be monitored as spacecraft motion causes the instrument field of view to move across the rings, providing a measure of ring optical thickness. These observations will be made of the portion of the rings which is in the shadow of Saturn. In addition, observations will be made with the instrument field of view pointed slightly off of the stellar target direction in order to measure the width of the forward scattered aureole, which is a measure of effective size of individual ring particles.

4. Interpretation of the Observations

ATMOSPHERES

In the absence of particulate matter or molecular absorbers in the atmospheres of Jupiter and Saturn, the intensity (or brightness) and polarization of light measured by the Voyager photopolarimeter would be dominated by molecular Rayleigh scattering and could be quite accurately predicted. The presence of particulate matter and molecular absorbers at different levels in these atmospheres causes two characteristic changes in the observed brightness of these bodies. First, the intensity as a function of wavelength is altered because of preferential absorption at specific wavelengths. An absorber may exist as a gaseous constituent of the atmosphere or as a component of particles suspended in the atmosphere. In cases where scattering results from non-absorbing particles whose size is comparable to the wavelength, differential efficiency with phase angle may cause intensity changes with wavelength at a given phase angle. In addition to the brightness variations with wavelength (color changes) caused by atmospheric absorbers and aerosols, the dependence of the brightness at a given wavelength upon viewing geometry is altered by the presence of non-Rayleigh scattering components. Both effects depend upon the altitude distribution of aerosols and absorbers in the Rayleigh scattering gas.

The measurement of the variation in brightness at a given wavelength with observational geometry is accomplished using the spacecraft scan platform pointing capability which allows a given region of Jupiter or Saturn to be viewed at several different phase, illumination, and viewing angles.

The analysis problem for photopolarimeter brightness measurements is to invert the variations in brightness with wavelength, phase or scattering angle, illumination angle, and viewing angle for each feature type to determine the vertical distribution of non-Rayleigh components (scatterers and absorbers) in the atmospheres of Jupiter and Saturn. In addition to altitude distributions, the approximate wavelength of any absorption features will be determined and the phase function of particulate scatterers will be measured.

For the atmospheres of Titan and other satellites the analytical capability of the PPS will be different. To make meaningful measurements, a first requirement is that the atmosphere must be sufficient to produce a scattered signal comparable to the surface scattering term. If this holds at any wavelength then some information about the atmosphere may be obtained. It is expected that the atmosphere of Titan may be

optically thick at the shorter wavelengths, but perhaps optically thin at the longer wavelengths, near 7500 Å.

Measuring polarization in addition to intensity is important for optically thick atmospheres, such as Jupiter and Saturn. Polarization effectively singles out first order scattering, since multiple scattering quickly reduces the polarizing effect observed from higher order scattering events. First-order scattering events are readily interpretable, and provide a basis for analyzing photopolarimeter data to identify non-Rayleigh scattering effects caused by atmospheric clouds. The photopolarimeter can effectively measure non-Rayleigh cloud scattering effects to a pressure level where the total of the incidence and exit optical paths is unity.

Approximate pressure levels probed by the photopolarimeter experiment vary from 0.1 to 10 bars, in the absence of clouds, on Jupiter when observing the illuminated disk at wavelengths of 2350 to 7500 Å, respectively. On Saturn the pressure range probed varies from 0.04 to 4.0 bars and on Titan from 0.005 to 0.5 bars. Bright limb, terminator, and occultation geometries extend the altitude range high into the atmosphere where the pressure is reduced by a factor of 100 in the case of Jupiter. The occurrence of clouds in these atmospheres will cause optical depth unity to occur higher in the atmosphere and limit the measurement pressure level. Variations in the pressure level reached by single scattered solar photons with illumination and observation angles provides the basis for the inversion of intensity and polarization data to find the vertical distribution of cloud particles. The values of illumination and observation angles control the atmospheric depth above which cloud scattering contributes to the intensity and polarization measured by the instrument. The observing plan is to vary, systematically the probing depth by geometry variations (e.g., Hord *et al.*, 1974) in order to determine the differential increase in cloud scattering with increased pressure.

The PPS atmospheric observations will include measurements in a methane absorption band (7270 Å) and in the nearby continuum (7500 Å). In conjunction with the polarimetry and multiple scattering computations for inhomogeneous atmospheres, these data will provide a detailed knowledge of atmospheric structure. For a complex vertical structure of cloud layers, the methane absorption provides a weighting function, varying with the geometry, so that a unique inversion will be possible. The many groundbased measurements of absorption lines and bands on Jupiter have not provided enough information to deduce a unique cloud structure. However, with the spatial resolution obtainable from the Voyager spacecraft, and the important advantage of being able to observe the same areas at different zenith angles and scattering angles, absorption band data will significantly augment the information on atmospheric structure obtainable from polarimetry.

Polarization analyses of planetary atmospheres have yielded detailed information for the clouds of Venus and Earth, planets for which essentially the full range of phase angles is available. For Venus, precise groundbased observations and detailed theoretical modeling permit an accurate determination of the shape and refractive

index of the cloud particles, their mean radius, the variance of the size distribution, and the cloud-top pressure.

Polarization analyses of terrestrial clouds have also been made, providing a test of the techniques on clouds for which other data are available. Figure 5 shows a comparison of theoretical curves to aircraft observations of a layer of maritime altostratus clouds. The figure illustrates the sensitivity of the polarization (but *not* the

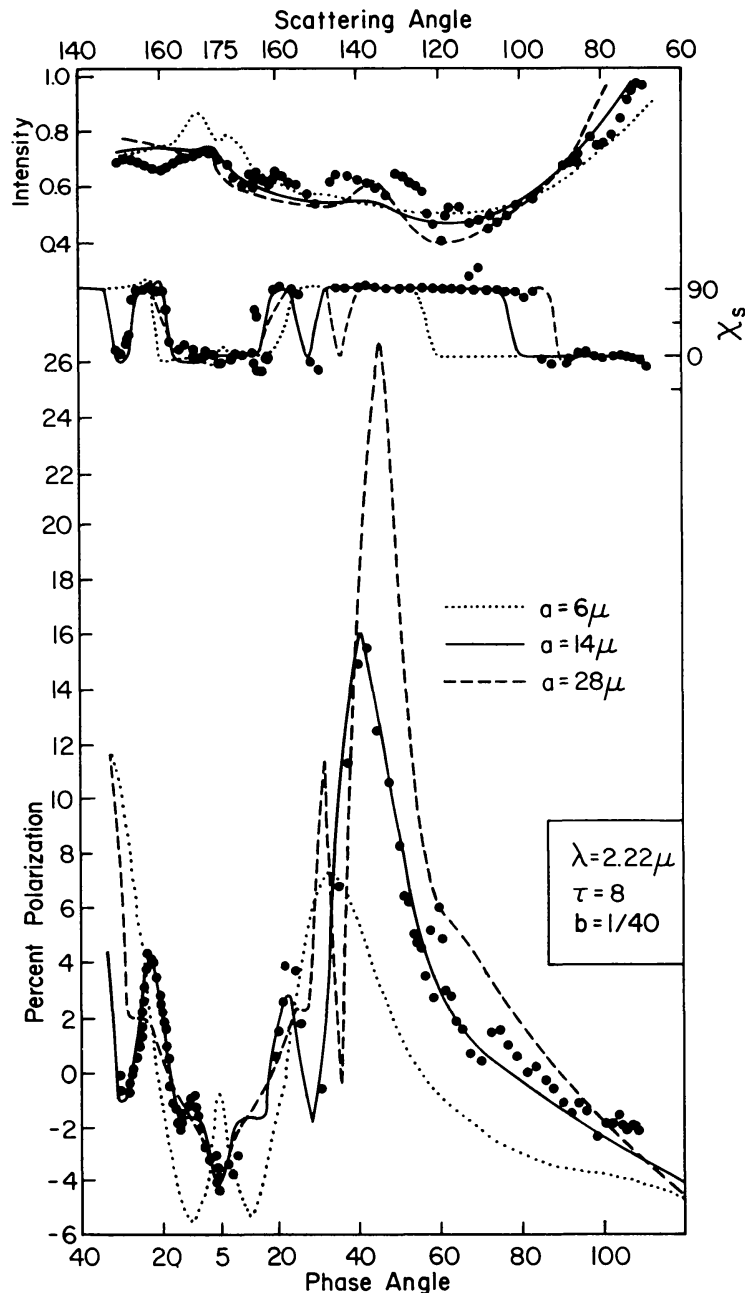


Fig. 5. Comparison of theoretical curves with observations (circles) of a layer of maritime altostratus clouds. The wavelength is 2.22μ . For the theoretical curves, the optical thickness is $\tau = 8$. The effective radius is a , and b is the effective variance of the size distribution. Note the primary rainbow at 40° phase angle (after Hansen and Coffeen, 1974).

intensity) to the mean particle size. Observations of cirrus clouds (Figure 6) illustrate the absence of the rainbow for nonspherical particles and the presence of positive polarization at intermediate phase angles for particles much larger than the wavelength.

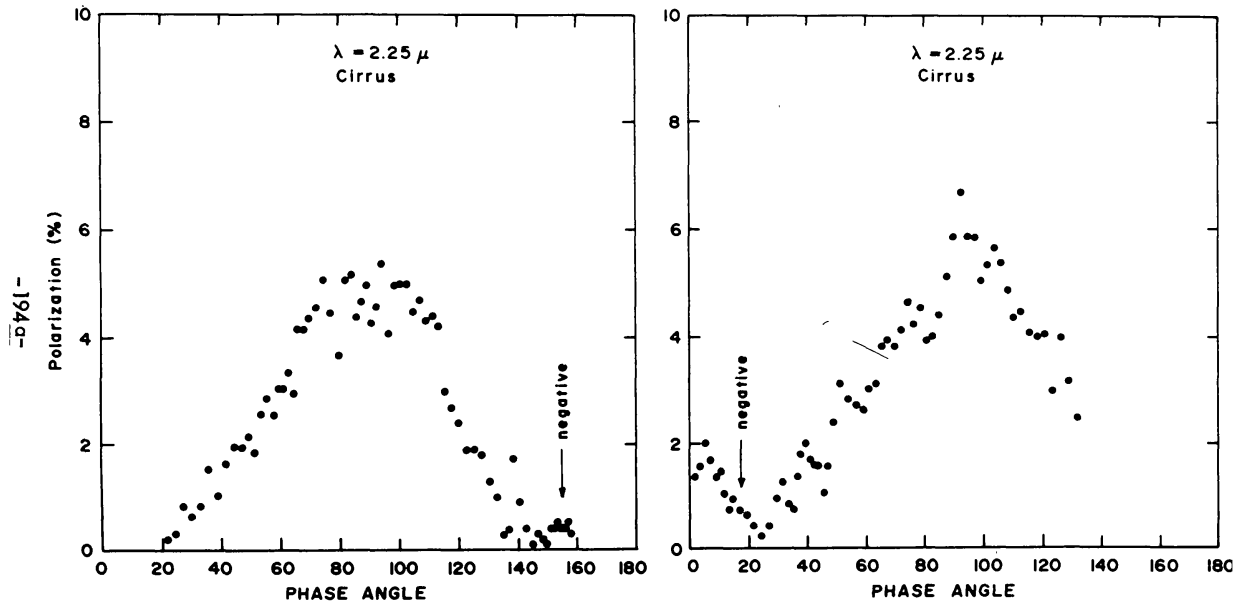


Fig. 6. Percent polarization of reflected sunlight observed at 2.25μ over a thick tropical cirrus system in the inter-tropical convergence zone. Note the absence of a cloudbow feature of strong positive polarization (after Coffeen and Hansen, 1972).

In the cases of Jupiter, Saturn, and Titan, polarization observations will be directed at acquiring data for particular planetary regions which are sufficiently small to have horizontal homogeneity. The necessary zenith and phase angle coverages will require repeatedly looking back at the given target region after the spacecraft has proceeded in its trajectory and/or the planet has rotated. If a belt or zone is assumed to be horizontally homogeneous, substantial zenith angle coverage and a small amount of phase angle coverage can also be obtained by scanning along the belt or zone. Broad coverage in phase angle is possible for the complete planet during cruise, and for detailed regions during a few days around closest approach.

Groundbased polarization observations of Jupiter are so restricted in phase angle (to $< 12^\circ$) that analyses of the data have yielded only a limited amount of information. The data are sufficient to show that the particles in the equatorial zone are nonspherical and $\approx 1\mu\text{m}$ in size (Kawabata and Hansen, 1975) and to indicate that the vertical distribution of particles in the equatorial zone is closer to a homogeneous mixture of cloud particles and gas than to gas above a dense cloud (cf. Figure 7). Measurements by Gehrels *et al.* (1969) of the polarization at the poles show that the cloud heights differ at the two poles and undergo temporal changes; Lyot (1929) also found strong cloud variation on a year-to-year basis.

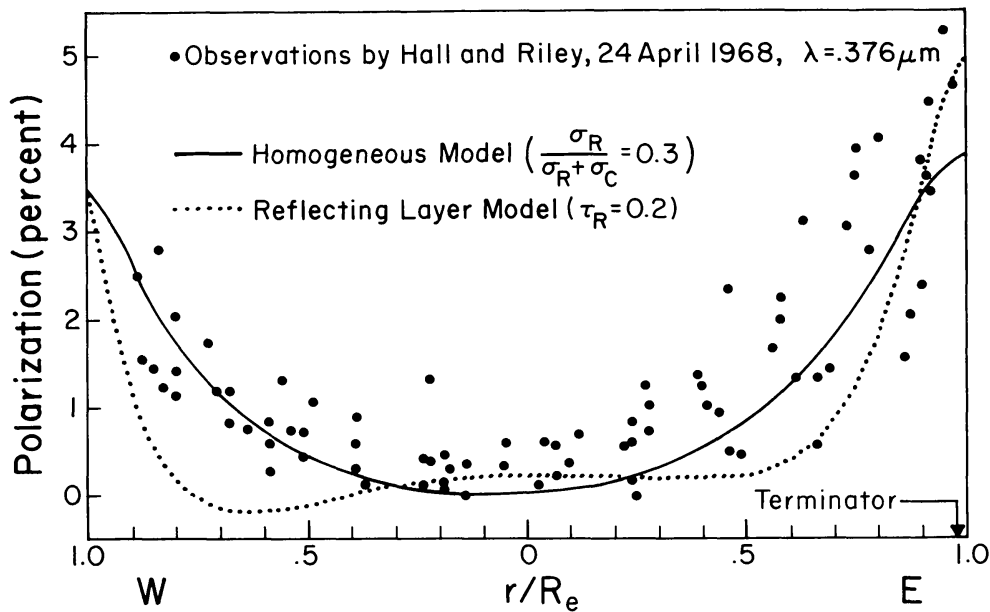


Fig. 7. Observed polarization along the Jovian equator (Hall and Riley, 1968). The homogeneous model corresponds to a photon mean free path ~ 30 km at 750 mb (where $\tau(\lambda = 0.55 \mu) = 1$). The reflecting layer model has a dense cloudtop at 430 mb.

Pioneers 10 and 11 each carried Imaging Photopolarimeters. The IPPS measurements were in two broad ($\sim 0.1 \mu\text{m}$) passbands centered at approximately 4400 \AA and 6400 \AA . Pioneer 10 (Coffeen, 1974) obtained polarization data with Jupiter well-resolved (> 20 resolution elements along a diameter) at 5 phase angles ($43, 103, 122, 141, 158^\circ$), while Pioneer 11 (Baker *et al.*, 1975) obtained such data at several phase angles in the range $38\text{--}140^\circ$. The polarization data analysis has so far been in terms of a model of Rayleigh scattering above a Lambertian cloud deck; this is useful for indicating relative cloud height variations (Figure 8). An alternative interpretation would be that the photon mean-free-path is shorter for regions such as the Red Spot. A choice between these interpretations will be possible from a detailed analysis of all the polarization data. It is also anticipated that the IPPS photometric data will yield useful information on the atmospheric structure of Jupiter (Tomasko, 1976).

With the PPS observations, including eight spectral bands between 2350 \AA and 7500 \AA and good phase angle and zenith angle coverage for a number of regions on Jupiter, Saturn, and Titan, a number of new and significant conclusions will be achieved. For the regions observed in detail, the vertical distribution of aerosols will be determined down to an optical depth of approximately unity. Differences such as those between hazy Venus-type clouds and sharp Earth-type clouds will be readily detectable. In the case of opaque clouds with sharp upper boundaries, an accurate measure of the cloud top pressure will be obtained. In the case of a hazy atmosphere, a measure of the particle number density will be obtained. From the polarization measurements it will be possible to distinguish between spherical, regular crystalline, and irregular particles. For spherical particles it will be possible to extract the particle refractive index and mean size; for regular crystalline particles to confirm or reject

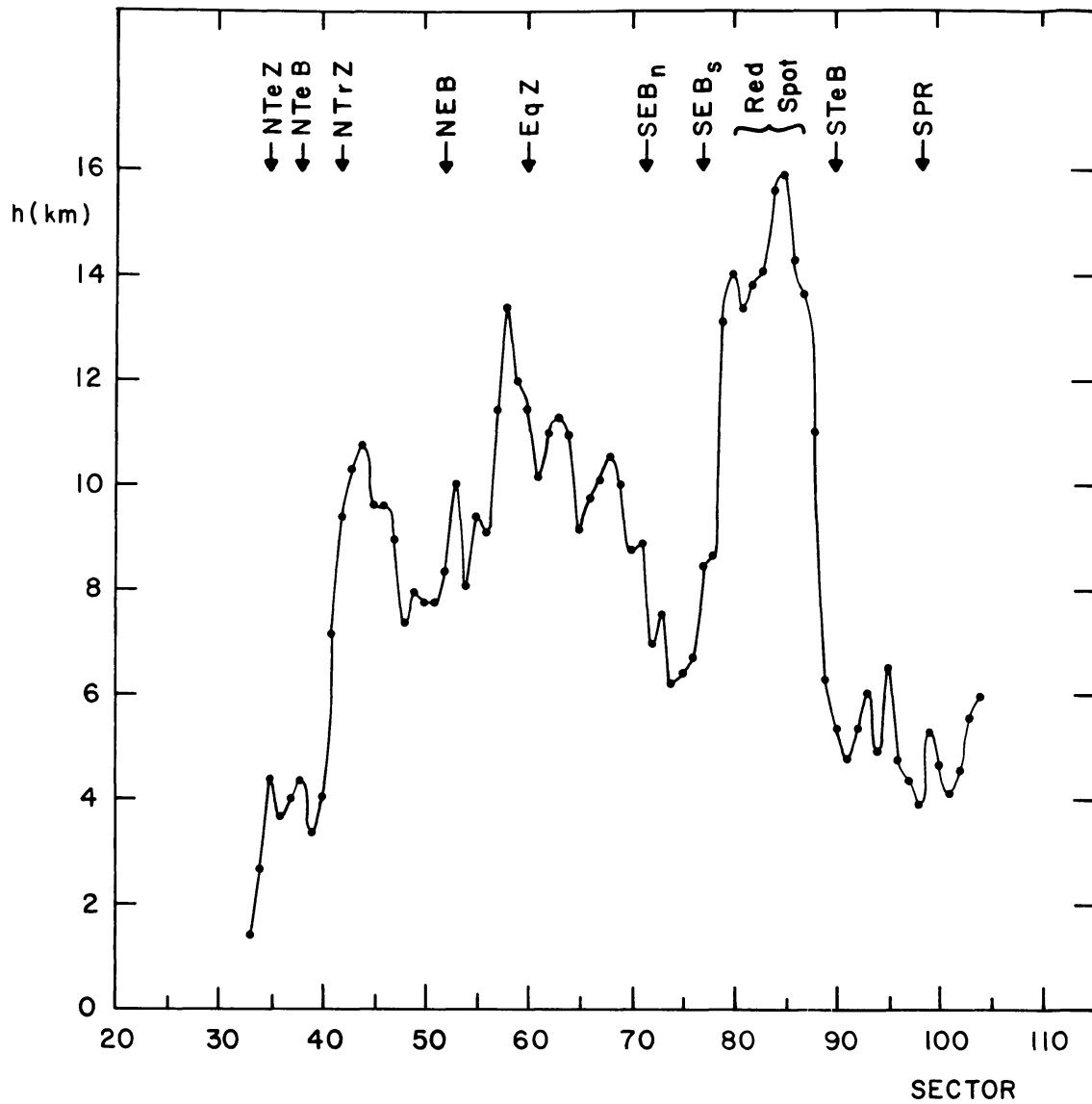


Fig. 8. Jupiter cloudtop altitudes (above the 650-mbar level) based on Pioneer 10 polarization measurements and a model for Rayleigh scattering above Lambert clouds (from Coffeen, 1974).

particular particle shape-refractive index combinations; and for irregular particles to determine whether the particles are larger than, of the order of, or smaller than the wavelengths of observation.

SATELLITES SURFACES

With the exception of their orbital parameters, the characteristics of the non-Galilean satellites and some of the Saturnian satellites are virtually unknown, a situation resembling that for the Martian satellites before the Mariner/Viking missions. For satellites which have detectable atmospheres, it will be possible to determine atmospheric densities and molecular scale heights and to detect the presence of atmospheric aerosols using the methods described in the previous

section. For all the satellites it will be possible to determine Bond albedos, surface textures, and probable surface compositions. For the satellites whose angular size significantly exceeds our smallest field of view, it will be possible to map the regional variations in surface properties. This information will be used to distinguish between theories for the origin and evolution of the satellites.

The importance of multi-color photometry and polarimetry of the satellites for studies of their surface properties has been demonstrated by recent studies of Phobos, Deimos, and the asteroids. McCord and Chapman (1975) have compared the spectra of nearly 100 asteroids, obtained by narrow-band photometry in the 0.33 to 1.1 μm region, with the spectral reflection curves of pulverized meteorites and other minerals, successfully identifying their composition. More recently, Pang *et al.* (1977) have used spectrophotometric data from the Mariner 9 Ultraviolet Spectrometer System and the Viking Lander cameras to show that the reflectance of Phobos is most consistent with a surface composition of carbonaceous chondrite.

Surface texture is strongly related to the depth of the negative branch of the polarization versus phase curve and the phase angle of zero crossing (Bowell and Zellner, 1974). From polarization measurements it will be possible to discriminate between surfaces consisting of bare rock, dust, frost deposits, ice, and impact-generated regolith.

As the Voyager spacecraft pass through the Jovian and Saturnian satellite systems, it will be possible to measure the satellites' phase functions in the range $0 \leq \psi \leq 160^\circ$ as well as their geometric albedoes. For the satellites whose diameters can be measured with the imaging system, it will be possible to calculate Bond albedoes and to calibrate the polarization-albedo relationship (Zellner and Gradie, 1976). Bond albedo measurements can be made on four Saturnian and at least five Jovian satellites (see Tables II and III). The Bond albedoes, together with infrared emission data, can give the bolometric albedo or energy budget for these satellites. Figure 9 shows the satellite phase angle coverage available on a typical Voyager Saturn flyby.

TABLE II
Jovian satellite surface studies

No.	Name	Surface polarim. ($\sim 10^\circ \sim 110^\circ$)	Bond albedo ($0^\circ - 160^\circ$)	Multiband photo-polarim. ($\pm 1\%$)	Regional surface comp. ($\geq 1.25^\circ$ ASD)	Global surface comp. ($\geq 0.09^\circ$ ASD)
J5		×	×	×		
J1	Io	×	×	×	3.5°	3.5°
J2	Europa	×	×	×		0.09°
J3	Ganymede	×	×	×	3.8°	3.8°
J4	Callisto	×	×	×	1.3°	1.3°
J6				×		
J7				×		
		4	4	7	3	4

TABLE III
Saturnian satellite surface studies

No.	Name	Surface polarim. ($\sim 10^\circ$, $\sim 110^\circ$)	Bond albedo ($0^\circ - 160^\circ$)	Multiband photo-polarim. ($\pm 1\%$)	Regional surface comp. ($\geq 1.25^\circ$ ASD)	Global surface comp. ($\geq 0.09^\circ$ ASD)
S10	Janus			×		
S1	Mimas	×	×	×		0.22°
S2	Enceladus	×	×	×		
S3	Tethys	×		×		0.44°
S4	Dione	×		×	3.3°	3.3°
S5	Rhea	×		×		0.40°
S6	Titan	×	×	×	5.0°	5.0°
S7	Hyperion	×		×		
S8	Iapetus	×	×	×		
S9	Phoebe	×		×		
		9	4	10	2	5

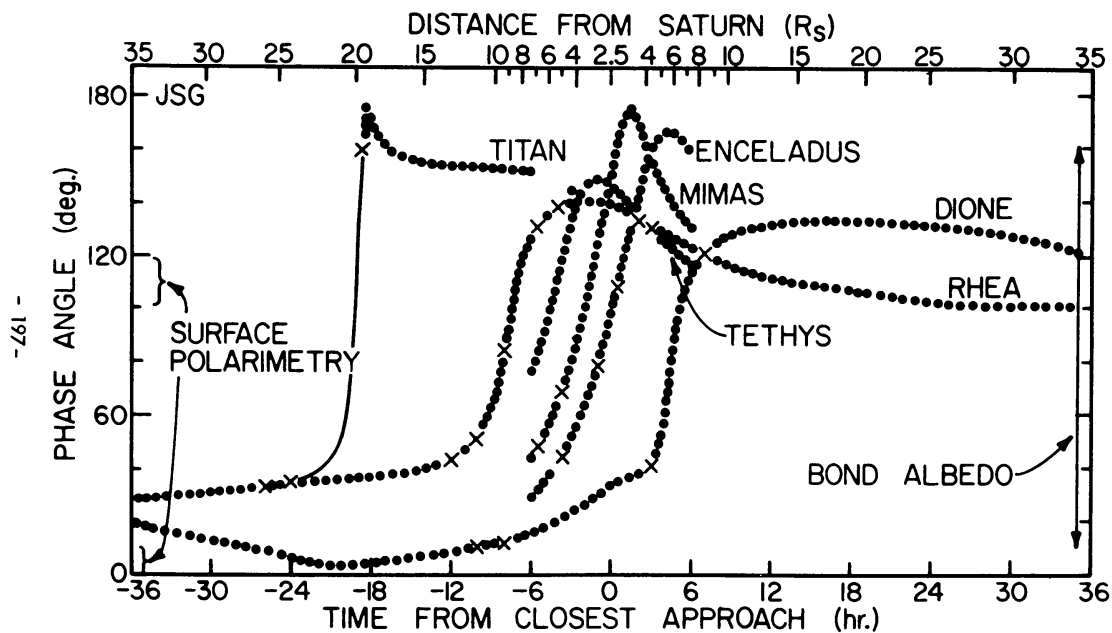


Fig. 9. Phase angle versus time for the Saturnian satellites as seen from the Voyager spacecraft. Crosses and solid lines indicate the planned observations.

An important objective of the Voyager mission is to obtain reliable size information for all satellites. Since all the irregular Jovian satellites are too small to be resolved by the imaging system, and too faint to be seen by the IR spectrometer, PPS albedo-polarization measurements seem to be the only feasible method of accomplishing this objective for these small bodies. Taking advantage of a wide range of phase angles at which observations can be made from Voyager, we can determine the

slope of the rising branch of the polarization curve and infer an albedo. Knowing the albedo and absolute brightness, we can infer the size of the satellite. The shape and rotational period of unresolved satellites can be deduced from their light curves. Polarization data, together with intensity measurements, can tell us whether the brightness variations are due to surface inhomogeneity or changing cross section.

Information on the surface composition of the non-Galilean satellites of Jupiter is badly needed to test contending theories on the formation of planetary satellites. The case of Amalthea is especially interesting. The radius (120 km) and albedo (0.1) of J5 (Rieke, 1975) are typical of an asteroid, and it does not fit in the orderly progression of the Galilean satellites. Amalthea revolves around Jupiter in a circular, equatorial orbit. If multi-spectral photometry of J5 does show that it is composed of carbonaceous chondrite, the evidence for planetary capture of asteroids would be compelling. With such new evidence, it would be difficult to maintain that Jupiter and Amalthea had a common origin, as still is possible in the case of Mars and Phobos.

The outer satellites of Jupiter can be divided into two groups: an inner group at about 11 million km with direct motion (J6, J7, J10) and an outer group at about 23 million km with retrograde motion (J8, J9, J11, J12). Surface compositional information can elucidate the question of common origins for these two groups of irregular satellites. Table II shows that the Voyager PPS is capable of obtaining accurate ($\pm 1\%$) photopolarimetric data on the Galilean satellites, J5, J6, and J7. Somewhat less accurate observations are possible for the other Jovian satellites. All Saturnian satellites will be observed with $\pm 1\%$ accuracy (see Table III).

Useful regional compositional data can be obtained when the angular semi-diameter (ASD) of a satellite significantly exceeds the smallest PPS field of view ($1/16^\circ$), i.e., hemispheric inhomogeneity at the same phase angle can be distinguished. This requirement is satisfied by the Galilean satellites (see Table II) and five of the saturnian satellites (see Table III). Regional surface compositional mapping via raster scanning is possible for only two or three satellites at each planet where an intentional close approach is realized.

Although the largest color variations for all the Galilean satellites occur in the ultraviolet, much of this spectral region is inaccessible to groundbased observers (Johnson and Pilcher, 1977). With a complement of four UV filters, the Voyager PPS is expected to open up this spectral region for detailed exploration. Preliminary UV photometry from OAO-2 has shown that such short wavelength observations are valuable. For example, the high reflectance of Io in the long wavelength region is approximated well by that of evaporite salts, but it requires a second substance, sulfur, to explain the sharp dropoff below about 500 nm (Fanale *et al.*, 1974). A mismatch still exists in the UV as the reflectance of sulfur turns up in the ultraviolet (Sill, 1973), while Io's reflectance continuously decreases with decreasing wavelength (Caldwell, 1975).

Multi-color photopolarimetry of the satellites of Jupiter and Saturn from the Voyager mission will provide baseline data for studies on future missions, as well as answering some of the questions posed above. The wide phase angle coverage from

Voyager will be especially valuable since the body-mounted scan platform on the Jupiter Orbiter/Probe (JOP), the next mission to Jupiter, will be limited to phase angles of approximately 85 to 135°.

TOROIDAL RINGS

McDonough and Brice (1973a, 1973b) first suggested that gas escaping from the atmosphere of a satellite of a major planet (Titan and Saturn in their case) might be unable to escape the planet's gravitational attraction and would thus form a toroidal or 'doughnut'-shaped ring around the planet at the distance of the satellite. Such a torus has indeed been discovered around Jupiter, associated with Io, as revealed by the atomic emissions of H I λ 1216, Na I λ 5893, K I λ 7699, and [S II] λ 6716 and λ 6731, which have been detected by Pioneer 10/11 and groundbased observers (Carlson and Judge, 1974; Brown and Chaffee, 1974; Kupo *et al.*, 1976).

During the far encounter phase of the Voyager mission we plan to scan the inner regions of the Jovian and Saturnian satellite systems to determine the distribution of Na I and K I and to search for emission from other atoms and ions, including Mg II λ 2800, the Ca II H and K lines, S II λ 4070, and Si I λ 2516.

Groundbased observations of Na-D line emission indicate Jupiter is surrounded by a disk-shaped cloud of sodium with an inner edge at $\sim 3R_J$ and an outer edge at $\sim 10R_J$, with surface brightnesses ranging from 0.5 to 20 kilo-Rayleighs. The most likely source of the sodium cloud is salts on the surface of Io which are bombarded by trapped particles in the Jovian magnetosphere.

With its largest field of view the photopolarimeter experiment sensitivity is approximately 200 counts sec^{-1} Rayleigh $^{-1}$ at 5893 Å. It can detect ~ 1 R of Na-D emission at radiation levels $< 5 \times 10^3$ 3-MeV electron $\text{cm}^{-2} \text{s}^{-1}$ (when the spacecraft is beyond $\sim 18R_J$) and ~ 1.5 kR at Io closest approach. If the Na-D emission has a $1/r^2$ dependence with distance from Io, we should be able to detect it out to approximately 140 Io radii.

We will map the distribution of Na around Io and the Jovian magnetosphere to provide information on the Na density, the production rate, the surface composition of Io, the flux of energetic particles, the structure of the magnetosphere, and the distribution of neutral material in the magnetosphere. Since sunlight scattered by the D₂ line is partially polarized, while the D₁ line is unpolarized (Chamberlain, 1961), polarization measurement of the Na-D emission give the D₁/D₂ line ratio which provides information on the temperature and optical thickness of the Na cloud.

Maps of the distribution of other atoms and ions will provide additional constraints on our models.

SATURN'S RINGS

The Rings of Saturn, unique in the Solar System, remain an enigma. Since their discovery more than 300 years ago, men have wondered about their origin, evolution, and dynamic motions as well as the properties of individual particles, such as their size, shape, albedo, structure, and composition. As an example of our

uncertainties, particle size estimates range from ice grains a few microns in diameter to kilometer-sized boulders in rolling contact. Suggested compositions range from frost-coated silicates to pure ice condensed from the solar wind.

Observations from the Voyager spacecraft should provide answers to most of these questions. The available groundbased data on Saturn's Rings consists primarily of surface brightness measurements as a function of wavelength, phase angle, ring tilt, and position in the rings. Stellar occultations by the rings occur occasionally, but are difficult to observe since the rings are much brighter than the stars which they occult.

The phase curves derived from these data have most successfully been treated by multiple scattering models in which the variables are the single scattering albedo and scattering phase function of the particles, the optical thickness and volume density (fraction of the total ring volume occupied by particles), and the appropriate geometric factors (Irvine and Lane, 1973).

The 'fine structure' in the surface brightness measurements of the rings, including the brightness decrease through Cassini's division, have been treated with dynamical ring models which consider the gravitational perturbations due to Mimas, Janus, and the other satellites of Saturn which act on the ring particles (Franklin *et al.*, 1971), as well as asymmetries in the gravitational field of Saturn, collisions between particles, and interactions with the solar wind.

Groundbased observations of the rings are hampered by scattered light from the disk of Saturn, atmospheric absorption in the ultraviolet part of the spectrum, seeing which is seldom better than 1 arcsec, and a limited range of viewing angles: phase angles $\leq 6^\circ$, ring tilt $\leq 26^\circ$. These limitations will be largely overcome by in situ observations from the Voyager spacecraft. Measurements will be obtained at phase angles up to 160° with 'ring tilts' from 0 to 90° . On the JSX mission the rings will subtend an angle of nearly 80° at closest approach, minimizing the problem of scattered light from Saturn. The other principal sources of the light of the night sky: airglow, light scattered in the Earth's atmosphere, and zodiacal light, will also be eliminated. At high galactic latitudes the surface brightness of the night sky should approach $V \approx 25.3$ magnitudes per square second of arc (Lillie, 1974), greatly enhancing the chances of detecting a D' ring outside ring A.

In the absence of atmospheric absorption the PPS will be able to obtain phase functions at eight wavelengths in the 2350 to 7500 Å region. It will also be possible to observe bright stars through the shadowed portion of the rings, as illustrated in Figure 10, to determine their optical depth as a function of wavelength. A few stars can be tracked from near the surface of Saturn to beyond ring A.

For some stars, the motion of the spacecraft will nearly cancel out the orbital velocity of the ring particles, permitting a search for occultations by individual particles. Particles larger than ~ 15 to 20 meters in diameter may be detected by this method.

At closest approach to Saturn the Voyager spacecraft will be nearly 7000 times closer than the Earth ever comes; thus, photometric scans across the illuminated

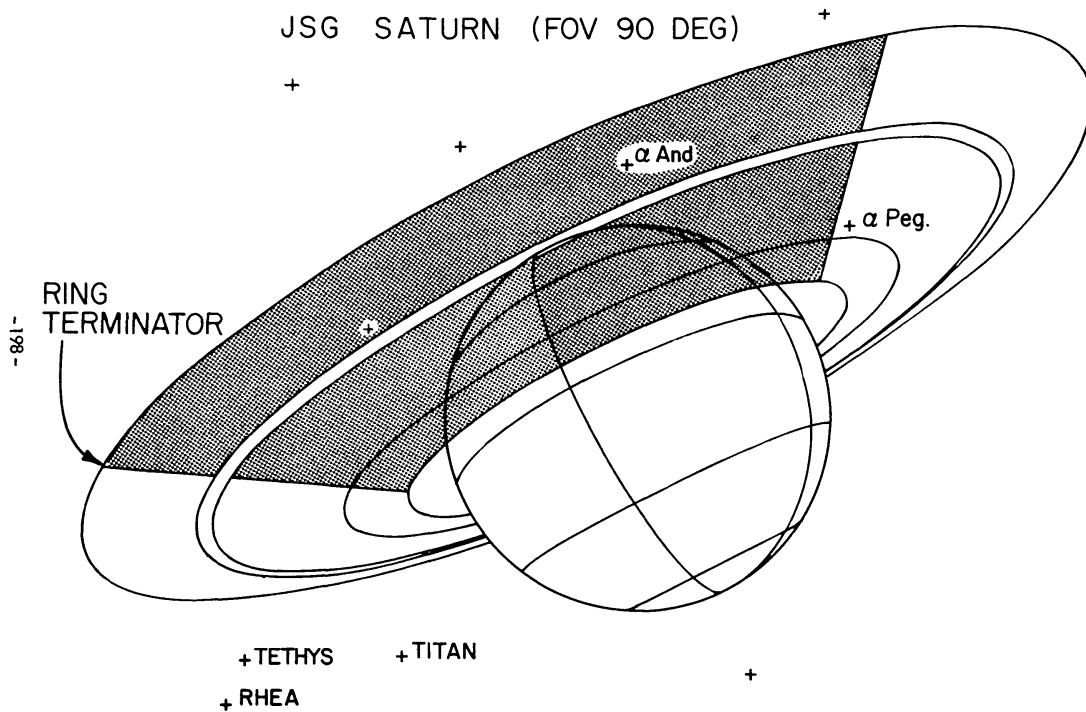


Fig. 10. The appearance of Saturn shortly after closest approach as the spacecraft passes through the shadow of Saturn. Stars appear to move from lower left to upper right behind the dark portion of the rings.

rings with the PPS $1/16^\circ$ FOV will have a resolution equivalent to 0.06 arcsec in a groundbased photograph.

During the time the Voyager spacecraft is in the shadow of Saturn it will be possible to measure the forward-scattering lobe of the ring particles in detail to complement measurements of the aureole around bright stars. The interpretation of these data will depend on the characteristic size of the ring particles. For sizes $< 10 \mu$ it will be possible to apply Mie scattering theory, as discussed in the atmospheres section, to determine particle size, shape, distribution, and probable composition. Particles larger than a few centimeters will be analyzed as an ensemble of individual satellites, in order to determine their surface texture and probable composition. In both cases it will be possible to determine albedoes and scattering phase functions. With thermal emission measurements from the IRIS experiment it will be possible to determine bolometric Bond albedoes for the ring particles.

By combining the data from all the remote sensing experiments on the Voyager spacecraft it will be possible to determine the ring's particle size distribution over several orders of magnitude.

In the 0.05 to $\sim 5 \mu$ range of radii the PPS experiment can determine sizes from variations in the wavelength dependence of the particles' scattering and extinction efficiencies. In the ~ 20 to 300μ region the intensity half-width of the aureole around bright stars is a measure of particle size; and, particles with radii > 10 m should individually occult stars seen through the shadowed portion of the rings.

RING ATMOSPHERE

The infrared reflection spectrum of the rings closely corresponds to the spectral reflectivity of water ice (Pilcher *et al.*, 1970). Blamont (1974) and Deneffeld have calculated the density and surface brightness of the OH cloud around the rings due to meteor bombardment, solar wind bombardment, sublimation, and subsequent photodissociation. Their predicted luminosity of OH, 10 Rayleighs, is readily detectable with the PPS experiment. Measurements of the luminosity and distribution of OH molecules would provide information on the composition, temperature, and meteor bombardment rate for the rings.

References

- Baker, A. L. and 15 co-authors: 1975, *Science* **188**, 468–472.
- Blamont, J.: 1974, in *The Rings of Saturn*, NASA SP-343, 125.
- Bowell, E. and Zellner, B.: 1974, in T. Gehrels (ed.), *Planets, Stars, and Nebulae studied with Photopolarimetry*, Univ. of Ariz. Press, Tucson, Ariz., p. 381.
- Brown, R. A. and Chaffee, F. H.: 1974, *Astrophys. J. Let.* **187**, L123.
- Caldwell, J.: 1975, *Icarus* **25**, 384.
- Carlson, R. W. and Judge, D. L.: 1974 *J. Geophys. Res.* **79**, 3623.
- Chamberlain, J. W.: 1961, *Physics of the Aurora and Airglow*, Academic Press, New York, p. 434.
- Coffeen, D. L.: 1974, *J. Geophys. Res.* **79**, 3645–3652.
- Coffeen, D. L. and Gehrels, T.: 1969, *Astron. J.* **74**, 433–445.
- Coffeen, D. L. and Hansen, J. E.: 1972, *Proc. of the Eighth International Symposium on Remote Sensing of Environment*, 515–522.
- Fanale, F. P., Johnson, T. V., and Matson, D. L.: 1974, *Science* **186**, 922.
- Franklin, F. A., Colombo, G., and Cook, A. F.: 1971, *Icarus* **15**, 80.
- Gehrels, T., Herman, B., and Owen, T.: 1969, *Astron. J.* **74**, 190–199.
- Hall, J. S. and Riley, L. A.: 1968, *Lowell Obs. Bull.* **7**, 83–92.
- Hansen, J. E. and Arking, A.: 1971, *Science* **171**, 669–672.
- Hansen, J. E. and Coffeen, D. L.: 1974, *Proc. of the Conf. on Cloud Physics of the Amer. Met. Soc.*, 350–356.
- Hord, C. W., Simmons, K. E., and McLaughlin, L. K.: 1974, *Icarus* **21**, 292–302.
- Irvine, W. M. and Lane, A.: 1973, *Icarus* **18**, 171.
- Johnson, T. V. and Pilcher, C. B.: 1977, *Proc. IAU Coll.* **28**.
- Kawabata, K. and Hansen, J. E.: 1975, *Bull. Amer. Astron. Soc.* **7**, 382 (abstract).
- Kupo, I., Mekler, Y., and Eviatar, A.: 1976, *Astrophys. J. Let.* **205**, L51.
- Lillie, C. F.: 1974, in *The Rings of Saturn*, NASA SP-343, 131.
- Lyot, B.: 1929, *Ann. Obs. Paris (Meudon)* **8**, 161 (in English as NASA TT F-187).
- McCord, T. B. and Chapman, C. R.: 1975, *Astrophys. J.* **197**, 781.
- McDonough, T. R. and Brice, N. M.: 1973a, *Nature* **242**, 513.
- McDonough, T. R. and Brice, N. M.: 1973b, *Icarus* **20**, 136.
- Pang, K. D., Pollack, J. B., Veverka, J., Lane, A. L., and Ajello, J. M.: 1977, *Bull. Amer. Astron. Soc.* **9**, (abstract).
- Pilcher, C. B., Chapman, C. R., Lebofsky, L. A., and Kieffer, H. H.: 1970, *Science* **167**, 1372.
- Rieke, G. H.: 1975, *Icarus* **25**, 333.
- Sill, G. T.: 1973, *Comm. Lunar Planet. Lab.* **10**, 1.
- Swendund, J. B., Kemp, J. C., and Wolstencroft, R. D.: 1972, *Bull. Amer. Astron. Soc.* **4**, 359.
- Tomasko, M. T.: 1976, in T. Gehrels (ed.), *Jupiter*, University of Arizona Press, Tucson, 1254 pp.
- Wolstencroft, R. D. and Rose, L. J.: 1967, *Astrophys. J.* **147**, 271.
- Zellner, B. and Gradie, J.: 1976, *Astron. J.* **81**, 281.